

Allen J. Bard^a and Royce W. Murray^{b,1}^aDepartment of Chemistry and Biochemistry, University of Texas, Austin, TX 78712; and ^bDepartment of Chemistry, University of North Carolina, Chapel Hill, NC 27599

For this special issue of PNAS, it seems appropriate to begin with a brief commentary on the path(s) leading to where the discipline of electrochemistry is today. The papers in this issue serve as a sampling of the current themes and directions; we thank the authors for their contributions. We should also point to a nice collection of historical perspectives gathered together by Leddy et al. (1).

The development of the electrochemistry discipline up to the 1960s was substantially that of the physical principles of describing electrochemical reactions and electrode reactions in which current or working electrode potential was controlled in some way. Those were aptly summarized in the classic 1954 text "New Instrumental Methods in Electrochemistry" (2). According to his introductory chapter, Delahay (2) wrote this influential text at the urging of the legendary I. M. Kolthoff, who prepared a preface to the book that stated "This book deserves a wide circle of friends." It was indeed very influential and added impetus for (then young) researchers like Bard and Murray to enter the discipline.

The introduction of flexible electrochemical equipment in the late 1950s, particularly including instruments based on the now-ubiquitous operational amplifier, unleashed an accelerated evolution of different ways to manipulate applied currents and potentials in electrochemical experiments. This evolution included the development by Nicholson and Shain of a technique first labeled as "stationary electrode polarography" but shortly afterward as "cyclic voltammetry" (CV) (3, 4). This was a very important development, because observation of the current pattern evoked by application of a single triangular wave potential scan, repeated at varied potential scan rates, allowed the informed researcher to deduce whether the current was controlled by mass transport, affected by a chemical reaction involving either the initial reactant or the product of the forward potential sweep, and involved reaction(s) of adsorbed species, as well as whether or not the reaction was electrochemically reversible. Such an enticing bonanza of information provided by the CV experiment provoked the present and continuing use of electrochemistry by a wide circle of researchers having a multitude of objectives. For example, CV has become an important technique that

complements spectroscopic techniques in studies of organic and inorganic species.

Analyses of CV responses and further probing of ever more complex and/or multiple chemical reactions accompanying electrochemical reactions encounter mathematical obstacles, centered on an inability to obtain explicit equation solutions of the mass transport processes coupled to the chemical processes. The necessity of using numerical solutions was a serious impediment until the effective aid of digital simulation was demonstrated (5) and commercial programs using implicit finite difference algorithms by Rudolph (6) in collaboration with Feldberg (7) became available.

The variety of electrochemical approaches to study chemical processes was boosted starting in the 1960s by combinations with spectroscopic measurements in which the working electrode is either optically "transparent" or highly reflecting, such that an incident light beam traverses the volume of reactant and product solution near the electrode surface (8, 9). This informs the electrochemical response with chemical structural information available from the spectra. "Spectroelectrochemistry" now encompasses a very wide range of spectral approaches that include reflectance, ellipsometry, internal reflection, surface plasmon resonance, second harmonic spectroscopy, and infrared and Raman spectroscopies, as well as X-rays. Spectroelectrochemical methods can also be devised in schemes in which the electrode reaction is monitored by the mass of its product (electrochemical quartz crystal microbalance), its magnetic properties (as in electron spin and NMR spectrometries), properties observed in high-vacuum experiments like electron spectrometry, and scanning probe methods. The book written by Bard and Faulkner (10) contains a summary of these developments.

A further development was small electrodes (i.e., microelectrodes), which were introduced by Adams in studying neurotransmitters *in vivo* and extended to even smaller sizes, sometimes called ultramicroelectrodes (UMEs), by Wightman and Fleischmann around 1980 (ref. 10, p. 169). The development of applications of UMEs was carried forward by Wightman and colleagues (11) and others to show that the combination of small currents and the associated loosening of tolerable solution resistance effects on electrochemical cell time constants, on the one hand lowered

the accessible time domains of electrochemical experiments and, on the other hand broadened the scope of usable low conductivity media. It is rare today to find electrochemical reports that do not take advantage of the virtues of UMEs. Current research leads onward into the land of nanoelectrodes, where ambitions of molecule-sized electrodes can be found.

In summary, the modern world of electrochemistry has been built on a range of experimental modalities and, in regard to its methods, may be said to be approaching "maturity." This maturity is not an end point, however, but one that enhances the ways in which new chemistry can be measured and understood. The span of chemical topics in the papers in this issue represents a sampling of that enhancement.

Electrochemical Properties of Modern Chemical Materials

In a recently described experiment called scanning electrochemical cell microscopy (12), the scanning probe is a double-barrel (θ) pipette filled with electrolyte solution, with each barrel containing a quasireference counterelectrode. The slightly protruding solution meniscus of the two filling solutions comprises a scanable electrochemical cell *ca.* 250 nm in diameter. In experiments described in this issue (13), contact by the protruding meniscus with one of a random network of single-walled carbon nanotubes (SWNTs), with the latter becoming a working electrode, allows interrogation of the SWNT electrochemical properties with reactions of a redox species dissolved in the pipette's filling solution [either the oxidizable ferrocenylmethyl trimethylammonium, FcTMA⁺, or the reducible ruthenium(III) hexamine, Ru(NH₃)₆³⁺]. Reactions at the SWNT occur under very large mass transport rates owing to the small SWNT radial dimension, such that the probe's heterogeneous electron transfer reaction rate constants become readily measurable. The observed values, $k_{\text{O}} = 9 \pm 2$ cm/s and $k_{\text{R}} = 4 \pm 2$ cm/s, respectively, were uniform along the sidewalls of the SWNTs, a central observation showing that the SWNT sidewalls (not merely the nanotube

Author contributions: A.J.B. and R.W.M. wrote the paper. The authors declare no conflict of interest.

¹To whom correspondence should be addressed. E-mail: rwm@unc.edu.

ends) are intrinsically reactive as tiny conducting nanotube surfaces.

Crooks and coworkers (14) have investigated the kinetics of the oxygen reduction reaction (ORR) in a microfluidic channel in which the oxygen-containing aqueous HClO_4 electrolyte solution flows over a pair of pyrolyzed photoresist carbon microbands used in a collector-generator mode (15). The generator microband bears a monolayer of dendrimers that encapsulate Pt_{147} or Pt_{55} nanoparticles. The combination of microchannel dimensions and solution flow rate yields a fast electrochemical reaction rate capability (mass transfer coefficients, k_t , as high as 0.5 cm/s) and access to dendrimer-encapsulated nanoparticle electrocatalytic activity under steady-state conditions. The experiments show that at low k_t , the effective number of electrons in the ORR differs for the two nanoparticle sizes ($n_{\text{eff}} = 3.7$ and 3.4 for Pt_{147} and Pt_{55} , respectively), and that at higher k_t , the ORR mass transfer-limited currents become significantly less than those for a four-electron reduction. The fraction of two-electron H_2O_2 reaction product, however, remains unchanged, signaling the possible intervention of a reaction rate step precedent to electron transfers (e.g., Pt nanoparticle- O_2 adsorption).

Molecular junctions are essentially modified electrodes familiar to electrochemists, in which the electrolyte is replaced by a conducting "contact." In the paper by McCreery and Bergren and colleagues (16), the molecular junction consists of a flat carbon electrode (composed of pyrolyzed photoresist films) that bears layers of covalently bonded nanoscopic molecular layers covered with a top contact of evaporated metal. The molecular layers are composed of seven different aromatic molecules deposited by the electrochemical reduction of diazonium reagents. The tunneling barriers for the different molecules prove to be much less different from one another than expected, which is explained as a reflection of very strong electronic coupling to the underlying carbon electrode.

Electrochemical Exploration of Biological Systems

Interest in and application of miniaturized electrochemical systems are further exemplified in work by White and Burrows and coworkers (17) on detection of DNA abasic lesion sites during the passage of DNA through the ion channel α -hemolysin embedded in a lipid bilayer. The detection is based on a momentary interruption of the ion current flowing through the channel that is induced in an applied voltage bias. The rate of DNA movement through such a channel is usually too fast for recording the passage of an individual abasic

site; in this case, the transit was retarded by selective attachment of a crown ether moiety, such that passage of individual sites could be detected.

In another paper, Wightman and colleagues (18) build on previous studies of dopamine and serotonin release in anesthetized rats by application of fast-scan CV at two implanted carbon fiber electrodes for simultaneous measurement of medial forebrain-stimulated release of serotonin and dopamine in the substantia nigra pars reticulata and nucleus accumbens brain regions, respectively. Electrode fouling by oxidation products of serotonin was successfully circumvented. The results show that distinctly differing processes control serotonin and dopamine release and uptake.

Fe-Fe and Ni-Fe hydrogenases are enzymes that catalyze rapid and efficient H^+/H_2 interconversion, a property otherwise exclusive to platinum metals. Examples from these two enzyme classes have been voltammetrically investigated by Armstrong and coworkers (19) as films on electrodes at varied temperatures. The voltammetry provides potential dependencies of the reaction rates of $\text{H}^+ \rightarrow \text{H}_2$ and $\text{H}_2 \rightarrow \text{H}^+$ for these "reversible catalysts," which are adsorbed on pyrolytic (edge plane) graphite electrodes, and delineates the differences between the Fe-Fe (better H_2 evolvers) and Ni-Fe (better H_2 oxidizers) hydrogenases in the context of electrocatalysis. Both contain FeS centers that mediate electron transfer between the protein surfaces and the buried catalytic sites. The study evolves a mathematical model of the catalytic schemes and shows that the catalytic bias is far greater for the Fe-Fe hydrogenases.

Koley and Bard (20) report on a continuation of scanning electrochemical microscopy (SECM) studies of the influx of a toxic species (menadione) and the export of the menadione-glutathione conjugate (thiodione) via the multidrug resistance pump (MRP1) in HeLa cells. By exporting thiodione, the cells can ameliorate its toxic effects; thus, by blocking the MRP1, the resistance of the cells to the agent is decreased. Measurements of influx and efflux by SECM with high temporal and spatial resolution were used to test two MRP1 blocking agents.

Barton and colleagues have extended (21) the capability of DNA-based sensors to electrocatalytic detection of targets using DNA films at low densities that bear methylene blue that is covalently tethered but flexible upon electron transfer with a hemoglobin electron sink. The spaces between the DNA chains in low-density films were backfilled and passivated by binding of 6-mercaptohexanol. A 10-s accumulation of chronocoulometric charge in the presence vs. absence of he-

moglobin was used to measure the difference in turnover numbers of the methylene blue-DNA ensemble. Function and sensitivity of the hemoglobin electrocatalysis scheme were tested by detection of a restriction enzyme.

The study by Mirkin and Amatore and coworkers (22) presents an analytical application of a nanoelectrode to mechanistic study of an important intracellular process, in which a platinumized nanoelectrode was used to penetrate a macrophage for detecting reactive oxygen and nitrogen species in the cytoplasm. Because these species are originally released inside the phagolysosome, their presence confirms that these lipophilic species can cross its membrane into the cytoplasm. The study relies on atomic force microscopy (AFM)-based modification of a nanoelectrode, which is used in mechanical stimulation/penetration of a macrophage, and detection there of extracellular and intracellular reactive oxygen and nitrogen species. This work should stimulate further applications of nanoelectrodes for intracellular electroanalytical measurements.

Electrochemical Methodology

A dual-mode imaging SECM experiment based on pyrolytic carbon nanoelectrodes is presented in the paper by Matsue and coworkers (23). To produce each topological data point of an image of the x - y plane, the (6.5- to 100-nm radius) nanoelectrodes are approached in the z direction until attaining a setpoint current that reflects a chosen degree of hindered (surface-shielded) diffusion of an added redox probe, such as $\text{Ru}(\text{NH}_3)_3^{3+}$. The z -direction position stops comprise the surface topology information. The nanoelectrode's z -direction motion is then arrested, and the nanoelectrode potential is adjusted to a value appropriate to detect and measure the concentration of a redox-active species, such as $\text{Ru}(\text{NH}_3)_6^{3+}$, O_2 , or some surface-emitted species. The small electrode dimension enables quick attainment of the steady-state, diffusion-limited current of the redox species. The nanoelectrode is then withdrawn, its potential is reset for detection of the redox probe, and it is repositioned in the x - y plane for recording of another pair of topology and redox current data points. Remarkably crisp images are produced for biological entities, such as membrane proteins on A431 cells, and of neurotransmitter emission from PC12 cells.

An investigation described by Stoddart and coworkers (24) provides a unique example of redox control over intramolecular electron transfer (IET) in an organic-based, mixed-valence bistable [2] rotaxane. Its dumbbell-shaped molecular architecture contains an electron-rich 1,5-dioxynaphthalene (DNP) unit linked to an

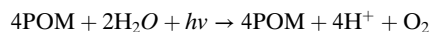
electron-poor phenylene-bridged bipyridinium (P-BIPY²⁺) unit. In the structure's ground state, a cyclobis(paraquat-*p*-phenylene) CBPQT⁴⁺ ring encircles the DNP unit. Reduction of the CBPQT⁴⁺ ring to its diradical dication CBPQT^{2(•+)} and of the P-BIPY²⁺ unit to its P-BIPY^{•+} radical cation leads to movement of the CBPQT^{2(•+)} ring along the dumbbell to surround the P-BIPY^{•+} unit, which, in turn, induces IET between the pyridinium redox centers of the P-BIPY^{•+} unit. Variable temperature electron paramagnetic resonance spectroscopy was used to assess the IET rate constant and activation energy as $k_{\text{ET}} = 1.33 \times 10^7 \text{ s}^{-1}$ and $\Delta G^\ddagger = 1.01 \text{ kcal mol}^{-1}$, respectively.

Photoelectrochemistry

Interest in solar energy-driven electrochemical water-splitting reactions (25) has promoted a focus on reactions that lead to the oxidation of water (26). Several of the contributions to this special issue deal with water oxidation reactions, and another deals with the materials aspects of photoelectrodes.

The study of redox reactions and ion transfers at liquid-liquid interfaces, called

interface between two immiscible electrolyte solutions (ITIES), is a well-developed area of electrochemistry. Work by Bond and colleagues (27, 28) exploits several liquid-liquid interfaces (water and either an ionic liquid or diethyl ether) for photoinduced interfacial reactions of polyoxometallate anions (POMs) that lead to oxidation of water and reduction of the polyoxometallate. The reduced polyoxometallate's overall general reaction with water is cast as



The evidence indicates that the reaction occurs at the solvent interface and can be induced by both artificial light and sunlight. The authors point to the possible role of differences in the structure of interfacial and bulk water; such differences have indeed been intensely studied, including by vibrational sum-frequency techniques and associated theory (29–31).

In another biphasic system (water, 1,2-dichloroethane), Girault and coworkers (32) elaborate on earlier work by Kunkely and Vogler (33) to show that

photolysis of osmocene (Cp₂Os) leads to a low-yield production of H₂ and oxidation of water in reactions involving formation of Cp₂Os dimers, such as [Cp₂Os^{III}—(H₂O)—Os^{III}Cp₂]²⁺. The ensuing O₂ released is intercepted by reduction by Cp₂Os hydride to yield hydrogen peroxide.

Kudo and colleagues (34) present information on photoelectrode preparation; in this case, a unique procedure is described to obtain thin films of the preferred scheelite phase of BiVO₄, which has known photocatalytic activity for water oxidation. The film is formed from calcining a fluorine tin oxide (FTO) electrode that was treated with precursor aqueous nitric acid solutions of Bi(NO₃)₃ and NH₄VO₃, leading to a BiVO₄ film that is several hundred nanometers thick. The photoelectrochemical activity of these films is evaluated, as is that of films that have been further modified and improved with a cobalt oxide. In connected experiments, water splitting to measured H₂ and O₂ products was demonstrated under visible light, using the BiVO₄ photoanode with a SrTiO₃/Rh photocathode without external applied potential bias.

- Leddy J, Birss V, Vanysek P (2004) *Historical Perspectives on the Evolution of Electrochemical Tools* (Electrochemical Society, Pennington, NJ).
- Delahay P (1954) *New Instrumental Methods in Electrochemistry* (Interscience Publishers, New York).
- Nicholson RS, Irving S (1964) Theory of stationary electrode polarography. Single scan and cyclic methods applied to reversible, irreversible, and kinetic systems. *Anal Chem* 36:706–723.
- Savéant JM (2006) *Elements of Molecular and Biomolecular Electrochemistry* (Wiley Interscience, Hoboken, NJ).
- Rudolph M (1991) A fast implicit finite difference algorithm for the digital simulation of electrochemical processes. *J Electroanal Chem* 314:13–22.
- Rudolph M, Reddy DP, Feldberg SW (1994) A simulator for cyclic voltammetric responses. *Anal Chem* 66: 589A–600A.
- Feldberg SW (1969) Digital simulation: A general method for solving electrochemical diffusion-kinetic problems. *Electroanal Chem* 3:199–296.
- Kuwana T, Darlington RK, Leedy DW (1964) Electrochemical studies using conducting glass indicator electrodes. *Anal Chem* 36:2023–2025.
- Murray RW, Heineman WR, O'Dom GW (1967) An optically transparent thin layer electrochemical cell. *Anal Chem* 39:1666–1668.
- Bard AJ, Faulkner LR (2001) *Electrochemical Methods: Fundamentals and Applications* (Wiley, New York), 2nd Ed.
- Dayton MA, Brown JC, Stutts KJ, Wightman RM (1980) Faradaic electrochemistry at microvoltammetric electrodes. *Anal Chem* 52:946–950.
- Ebejer N, Schnippering M, Colburn AW, Edwards MA, Unwin PR (2010) Localized high resolution electrochemistry and multifunctional imaging: Scanning electrochemical cell microscopy. *Anal Chem* 82: 9141–9145.
- Güell AG, et al. (2012) Quantitative nanoscale visualization of heterogeneous electron transfer rates in 2D carbon nanotube networks. *Proc Natl Acad Sci USA* 109:11487–11492.
- Dumitrescu I, Crooks RM (2012) Effect of mass transfer on the oxygen reduction reaction catalyzed by platinum dendrimer encapsulated nanoparticles. *Proc Natl Acad Sci USA* 109:11493–11497.
- Dumitrescu I, Yancey DF, Crooks RM (2012) Dual-electrode microfluidic cell for characterizing electrocatalysts. *Lab Chip* 12:986–993.
- Sayed SY, Fereiro JA, Yan H, McCreery RL, Bergren AJ (2012) Charge transport in molecular electronic junctions: Compression of the molecular tunnel barrier in the strong coupling regime. *Proc Natl Acad Sci USA* 109:11498–11503.
- An N, Fleming AM, White HS, Burrows CJ (2012) Crown ether–electrolyte interactions permit nanopore detection of individual DNA basic sites in single molecules. *Proc Natl Acad Sci USA* 109:11504–11509.
- Hashemi P, et al. (2012) Brain dopamine and serotonin differ in regulation and its consequences. *Proc Natl Acad Sci USA* 109:11510–11515.
- Hexter SV, Grey F, Happe T, Climent V, Armstrong FA (2012) Electrocatalytic mechanism of reversible hydrogen cycling by enzymes and distinctions between the major classes of hydrogenases. *Proc Natl Acad Sci USA* 109:11516–11521.
- Koley D, Bard AJ (2012) Inhibition of the MRP1-mediated transport of the menadione-glutathione conjugate (thiodione) in HeLa cells as studied by SECM. *Proc Natl Acad Sci USA* 109:11522–11527.
- Pheney CG, Guerra LF, Barton JK (2012) DNA sensing by electrocatalysis with hemoglobin. *Proc Natl Acad Sci USA* 109:11528–11533.
- Wang Y, et al. (2012) Nanoelectrodes for determination of reactive oxygen and nitrogen species inside murine macrophages. *Proc Natl Acad Sci USA* 109:11534–11539.
- Takahashi Y, et al. (2012) Topographical and electrochemical nanoscale imaging of living cells using voltage-switching mode scanning electrochemical microscopy. *Proc Natl Acad Sci USA* 109:11540–11545.
- Barnes JC, et al. (2012) Mechanically induced intramolecular electron transfer in a mixed-valence molecular shuttle. *Proc Natl Acad Sci USA* 109:11546–11551.
- Liu F, et al. (2008) Mechanisms of water oxidation from the blue dimer to photosystem II. *Inorg Chem* 47: 1727–1752.
- Nakagawa T, Beasley CA, Murray RW (2009) Highly efficient electro-oxidation of water near its reversible potential by a mesoporous IrO₂ nanoparticle film. *J Phys Chem C Nanomater Interfaces*, 113:12958–12961, (lett).
- Bernadini G, Wedd AG, Zhao C, Bond AM (2012) Photochemical oxidation of water and reduction of polyoxometalate anions at interfaces of water with ionic liquids or diethylether. *Proc Natl Acad Sci USA* 109: 11552–11557.
- Bernardini G, Zhao C, Wedd AG, Bond AM (2011) Ionic liquid-enhanced photooxidation of water using the polyoxometalate anion [P₂W₁₈O₆₂]⁶⁻ as the sensitizer. *Inorg Chem* 50:5899–5909.
- Hore DK, Walker DS, MacKinnon GL (2008) Water at hydrophobic surfaces: When weaker is better. *J Am Chem Soc* 130:1800–1801.
- Hore DK, Walker DS, MacKinnon L, Richmond GL (2007) Molecular structure of the chloroform–water and dichloromethane–water interfaces. *J Phys Chem C Nanomater Interfaces* 111:8832–8842.
- Walker DS, Moore FG, Richmond GL (2007) Vibrational sum-frequency spectroscopy and molecular dynamics simulations of the carbon tetrachloride–water and 1,2-dichloroethane–water interfaces. *J Phys Chem C Nanomater Interfaces* 111:6103–6112.
- Ge P, et al. (2012) Biphasic water splitting by osmocene. *Proc Natl Acad Sci USA* 109:11558–11563.
- Kunkely H, Vogler A (2009) Water splitting by light with osmocene as photocatalyst. *Angew Chem Int Ed* 48:1685–1687.
- Jia Q, Iwashina K, Kudo A (2012) Facile fabrication of an efficient BiVO₄ thin film electrode for water splitting under visible light irradiation. *Proc Natl Acad Sci USA* 109:11564–11569.